Topoisomerase poisons differentially activate DNA damage checkpoints through ataxia-telangiectasia mutated–dependent and –independent mechanisms

Wai Yi Siu, Anita Lau, Talha Arooz, Jeremy P.H. Chow, Horace T.B. Ho, and Randy Y.C. Poon

Department of Biochemistry, Hong Kong University of Science and Technology, Clear Water Bay, Kowloon, Hong Kong

Abstract

Camptothecin and Adriamycin are clinically important inhibitors for topoisomerase (Topo) I and Topo II, respectively. The ataxia-telangiectasia mutated (ATM) product is essential for ionizing radiation-induced DNA damage responses, but the role of ATM in Topo poisons-induced checkpoints remains unresolved. We found that distinct mechanisms are involved in the activation of different cell cycle checkpoints at different concentrations of Adriamycin and camptothecin. Adriamycin promotes the G_1 checkpoint through activation of the p53-p21$^{CIP1/WAF1}$ pathway and decrease of pRb phosphorylation. Phosphorylation of p53(Ser20) after Adriamycin treatment is ATM dependent, but is not required for the full activation of p53. The G_1 checkpoint is dependent on ATM at low doses but not at high doses of Adriamycin. In contrast, the Adriamycin-induced G_2 checkpoint is independent on ATM but sensitive to caffeine. Adriamycin inhibits histone H3(Ser10) phosphorylation through inhibitory phosphorylation of CDC2 at low doses and down-regulation of cyclin B1 at high doses. The camptothecin-induced intra-S checkpoint is partially dependent on ATM, and is associated with inhibitory phosphorylation of cyclin-dependent kinase 2 and reduction of BrdUrd incorporation after mid-S phase. Finally, apoptosis associated with high doses of Adriamycin or camptothecin is not influenced by the absence of ATM. These data indicate that the involvement of ATM following treatment with Topo poisons differs extensively with dosage and for different cell cycle checkpoints. [Mol Cancer Ther 2004;3(5):621–32]

Introduction

DNA damage checkpoints operate throughout the cell cycle to maintain genetic integrity. These checkpoints ensure that damaged DNA are not replicated or segregated to the daughter cells until repaired. One of the mechanisms through which DNA damage checkpoints delay cell cycle progression is through inhibition of cyclin-cyclin-dependent kinase (CDK) complexes. Cyclin-CDK complexes are key regulators of the cell cycle: cyclin D-CDK4/6 for G_1 progression, cyclin E-CDK2 for G_1-S transition, cyclin A-CDK2 for S phase progression, and cyclin A/B-CDC2 for M phase entry (reviewed in Ref. 1).

Ataxia-telangiectasia mutated (ATM) is mutated in the human genetic disorder ataxia-telangiectasia (AT) (reviewed in Ref. 2). AT is characterized by progressive cerebellar ataxia, immune dysfunction, cancer predisposition, and radiosensitivity (reviewed in Ref. 3). AT cells exhibit an enhanced radiosensitivity, radioresistant DNA synthesis, and chromosomal instability. ATM encodes a product related to phosphatidylinositol 3 kinases and phosphorylates several substrates involved in the DNA damage checkpoints. It is well established that ATM is essential for p53 accumulation and the DNA damage checkpoints in response to ionizing radiation-induced double-strand breaks. On the other hand, p53 induction in AT cells was normal after other types of DNA damage like UV irradiation, suggesting the involvement of the ATM-related protein ATR (reviewed in Ref. 4). In agreement with this, deletion of ATR leads to loss of the ionizing radiation-induced G_2 checkpoint (5, 6). In addition to acting through the above checkpoint pathways, ATM also acts on a parallel pathway involving the trimeric protein complex MRE11-NBS1-RAD50 (reviewed in Ref. 7).

DNA damage checkpoints in G_1 and S phase comprise of rapid responses involving cyclin D1 and CDC25A, and a relatively slower response involving p53. Cyclin D1 is rapidly degraded by ubiquitin/proteasome-dependent mechanisms after DNA damage, resulting in the redistribution of the CDK inhibitors p21$^{CIP1/WAF1}$ and p27^{KIP1} from cyclin D1-CDK4/6 to cyclin A/E-CDK2 (8–10). DNA damage also promotes the destruction of CDC25A through phosphorylation of CDC25A by ATM, CHK1, and CHK2 (11, 12). This prevents the dephosphorylation of Thr14/Tyr15 in CDK2 and promotes radioresistant DNA synthesis. A slower G_1 DNA damage checkpoint is carried out by p53. MDM2, a transcriptional target of p53, abolishes p53 functions by direct interaction (reviewed in Ref. 13). Several DNA damage-induced protein kinases, including ATM, ATR, CHK1, and CHK2 phosphorylate p53 (including Ser9, Ser15, Ser20, and Ser46) and inhibit the binding to MDM2 (14–17). Activated p53 in turn promotes the expression of its downstream target p21$^{CIP1/WAF1}$, resulting in cell cycle arrest.

The G$_2$ DNA damage checkpoint exerts its effects in part through the inhibitory phosphorylation of CDC2 (reviewed in Ref. 18). On DNA damage, ATM/ATR phosphorylates and activates CHK1/CHK2, which in turn phosphorylates CDC25C on Ser216. This creates a 14-3-3 binding site and inactivates the phosphatase activity of CDC25C (19, 20). Destruction of another member of the CDC25 family, CDC25A, is also necessary to prevent damaged cells from entering mitosis (21). Similarly, WEE1, the protein kinase that opposes the action of CDC25 by phosphorylating CDC2 on Tyr15, can also be phosphorylated and activated by CHK1 (22).

Inhibitors of topoisomerase (Topo) I and Topo II are clinically important chemotherapeutic agents (reviewed in Ref. 23). The majority of Topo inhibitors interfere with the religation step in the normal action of the enzymes, which leads to a stabilization of cleavable Topo-DNA complexes. This produces single-strand DNA breaks in the case of Topo I or double-strand breaks in the case of Topo II. Single-strand breaks caused by Topo I inhibition are converted into double-strand breaks in the course of DNA replication. Topo inhibitors are thus generally regarded as radiomimetic chemicals. Similar to ionizing radiation, several radiomimetic chemicals (including neocarcinostatin and bleomycin) induce p53 responses in an ATM-dependent manner (24, 25). However, the role of ATM in DNA damage responses to Topo inhibitors is less conclusive. Activation of p53 in response to camptothecin (a Topo I poison) and etoposide (a Topo II poison) is independent of ATM (25, 26). Similarly, activation of CHK2 by Topo II inhibitors Adriamycin and etoposide is also independent of ATM (26, 27). On the other hand, activation of p53 and CHK2 by the Topo II inhibitor genistein is ATM dependent (26, 27), and the S phase DNA damage checkpoint induced by Topo I inhibitors is dependent on CHK1 and ATR (28, 29). In this report, we characterize the molecular responses to Topo I and Topo II poisons in more detail, in particular with reference to the relationship with ATM. For DNA damage checkpoints in G$_1$ and S, we evaluated whether the activation of p53, induction of p21$^{CIP1/WAF1}$, inhibitory phosphorylation of CDK2, and DNA replication are affected by caffeine or are defective in cells without ATM. For the G$_2$ DNA damage checkpoint, the inhibitory phosphorylation of CDC2, down-regulation of cyclin B1, and histone H3 phosphorylation were investigated. We found that all DNA damage checkpoints are sensitive to caffeine after treatment with low doses but not high doses of Topo poisons. ATM-dependent mechanisms partly accounted for the G$_1$ checkpoint and S checkpoint, but are not responsible for the G$_2$ DNA damage checkpoint triggered by Topo poisons.

Materials and Methods
Materials
All reagents were obtained from Sigma-Aldrich (St. Louis, MO) unless stated otherwise.

Cell Culture
HeLa (human cervical carcinoma) and HepG2 (human hepatoblastoma) were obtained from the American Type Culture Collection (Manassas, VA). Normal human lymphoblastoid cells (GM03798), and AT lymphoblastoid cells (GM03189) were obtained from Coriell Cell Repositories (Camden, NJ). Cells were propagated under conditions as suggested by the suppliers. Synchronization by double thymidine block and by nocodazole was as described previously (30). Cell-free extracts were prepared as described (9). Unless stated otherwise, cells were treated with the following reagents at the indicated final concentration: Adriamycin (200 ng/ml), caffeine (5 μM), camptothecin (700 nM), hydroxyurea (1.5 mM), and nocodazole (0.1 μg/ml).

Flow Cytometry and BrdUrd Incorporation Analysis
Flow cytometry after propidium iodide staining was performed as described previously (31). For flow cytometry after staining with antibodies, cells were harvested by trypsinization, fixed in ice-cold 80% ethanol, and washed twice with PBST (PBS supplemented with 0.5% v/v Tween 20 and 0.05% w/v BSA). The cell pellet was resuspended in the residue buffer and incubated with 1 μg of primary antibody at 25°C for 30 min. The cells were washed twice with PBST, resuspended in the residue buffer, and incubated with 2.5 μl of FITC-conjugated anti-mouse IgG or FITC-conjugated anti-rabbit IgG antibodies (DAKO, Glostrup, Denmark) at 25°C for 30 min. After washing once in PBST, the cells were processed for propidium iodide staining and two-dimensional flow cytometry analysis. Analysis of BrdUrd incorporation was performed as described previously (32).

Phosphatase Treatment and Histone H1 Kinase Assays
The glutathione *S*-transferase (GST)-human CDC25A construct was a gift from Katsumi Yamashita (Kanazawa University, Kanazawa, Japan). Expression of recombinant proteins in bacteria and purification with GSH-agarose chromatography were as described previously (9). Immunoprecipitates were incubated with 1 μg of GST-fusion proteins in phosphatase buffer [10 mM HEPES (pH 7.2), 25 mM KCl, 10 mM NaCl, 1.1 mM MgCl$_2$, 0.1 mM EDTA, 0.1 mM DTT] at 25°C for 30 min. After washing in kinase buffer (80 mM Na β-glycerophosphate, 20 mM EGTA, 15 mM MgOAc, 1 mM DDT), the histone H1 kinase activity was assayed as described previously (33). Phosphorylation was quantified with a PhosphorImager (Amersham Biosciences, Piscataway, NJ).

Antibodies and Immunological Methods
Immunoblotting and immunoprecipitation were performed as described previously (9). Rat monoclonal antibodies YL1/2 against tubulin, monoclonal antibodies E23 against cyclin A2, A17 against CDC2, AN4.3 against CDK2, and IF8 against pRb were gifts from Tim Hunt and Julian Gannon (Cancer Research UK). Polyclonal antibodies against CDK2 (34) were from Katsumi Yamashita (Kanazawa University). Monoclonal antibodies DO1 against p53 (sc-126), GNS1 against cyclin B1 (sc-245), HE12 against cyclin E (sc-247), caspase-3 (sc-7272), and polyclonal antibodies against p21$^{CIP1/WAF1}$ (sc-397) and phospho-histone H3 (Ser10) (sc-8656R) were obtained from Santa Cruz Biotechnology (Santa Cruz, CA). Antibodies against phospho-p53(Ser20) were obtained from Cell Signaling Technology (Beverly, MA).

Results

Different Mechanisms Are Involved in Cell Cycle Inhibition at Different Concentrations of Topo Poisons

To study the molecular basis of DNA damage responses to Topo poisons, we initially employed a widely used cell line HepG2 (contains wild-type p53 and pRb; Ref. 35). Figure 1A shows that p53 accumulated in response to both camptothecin (a Topo I inhibitor) and Adriamycin (a Topo II inhibitor) in a dose-dependent manner. Accumulation of p53 correlated with the phosphorylation of Ser20, a site that is phosphorylated through the ATM/ATR-CHK1/CHK2 pathway (16, 36, 37). The reduction of p53 at the highest camptothecin concentration used (*lane 6*) was probably due to extensive cell death. As expected, the p53 target p21$^{CIP1/WAF1}$ was also induced by camptothecin and Adriamycin.

Interestingly, inactivation of CDC2 through Thr14/Tyr15-inhibitory phosphorylation (as indicated by the slower migrating forms; Ref. 38) occurred at drug concentrations below that induced p53. At higher concentrations of Adriamycin/camptothecin, CDC2 was inactivated not by phosphorylation, but through the loss of cyclin A and cyclin B1. The constant level of tubulin indicated that the decrease of mitotic cyclins was not due to general protein degradation. Unlike CDC2, inhibitory phosphorylation of CDK2 does not manifest as mobility shift on SDS-PAGE. We found that the kinase activities of CDK2 were inhibited after treatments with Adriamycin and camptothecin (Fig. 1B). Inactivation of CDK2 was due to inhibitory phosphorylation because it could be reactivated with bacterially expressed CDC25A (Fig. 1C).

Flow cytometry analysis at 24 h after drug addition (the time for about one normal cell cycle in HepG2) indicated that different doses of Topo inhibitors triggered different types of cell cycle delay. As expected, camptothecin predominantly arrested cells during S phase (and some G_2 arrest at low concentrations) (Fig. 2A). High concentrations of camptothecin arrested HepG2 throughout S phase and with 2N DNA content (it is not possible to distinguish G_1 and early S phase arrests with these analyses). The inhibition of DNA synthesis was verified by BrdUrd labeling (see later). In contrast, Adriamycin treatment triggered arrest in both G_1 and G_2. An S phase delay was progressively introduced at higher concentrations of Adriamycin, resulting in stalling throughout the cell cycle. Both G_1 and G_2 arrest were stable, as the cell cycle profiles were not altered up to 72 h (Fig. 2B).

To study the temporal relationship between p53 activation and cyclin down-regulation, cells were treated with the same dose of Adriamycin and harvested at different time points (Fig. 2C). We found that when cells were treated with 200 ng/ml of Adriamycin, p53 was rapidly phosphorylated
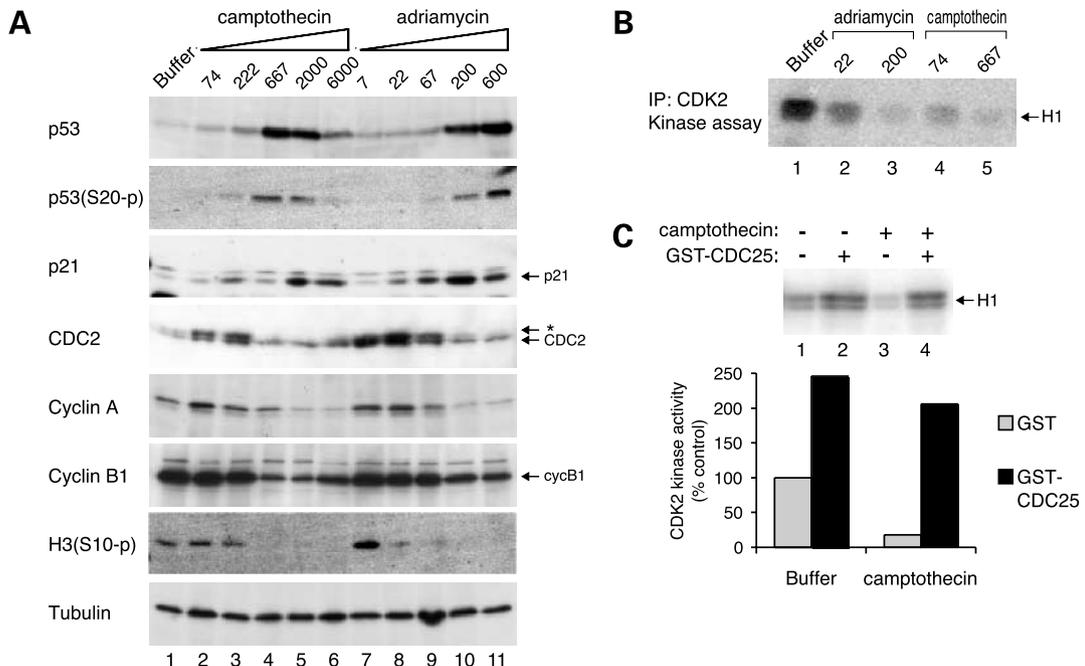

Figure 1. Different doses of Topo poisons differentially modulate cell cycle regulators. **A,** inactivation of CDC2 and activation of p53 are triggered by different concentrations of Topo poisons. HepG2 cells were mock treated (*lane 1*) or treated with the indicated concentrations of camptothecin (nM) or Adriamycin (ng/ml) for 24 h. Cell extracts were prepared and were subjected to immunoblotting for p53, Ser20-phosphorylated p53, p21$^{CIP1/WAF1}$, CDC2, cyclin A, cyclin B1, and Ser10-phosphorylated histone H3 as indicated. Immunoblotting for tubulin indicates similar sample loadings. The *asterisk* indicates the position of the slower migrating, Thr14/Tyr15-phosphorylated forms of CDC2. **B,** inactivation of CDK2 after DNA damage. HepG2 cells were mock treated or treated with the indicated doses of Adriamycin (ng/ml) or camptothecin (nM). Cells were harvested 24 h later and the histone H1 kinase activities associated with CDK2 were assayed as described in Materials and Methods. **C,** reactivation of CDK2 by recombinant CDC25A. HepG2 cells were either mock treated or treated with 74 nM camptothecin for 24 h before cell extracts were prepared. CDK2 was immunoprecipitated and incubated with either GST or GST-CDC25A as described in Materials and Methods. Histone H1 kinase activity was assayed and phosphorylation was quantified with a PhosphorImager.
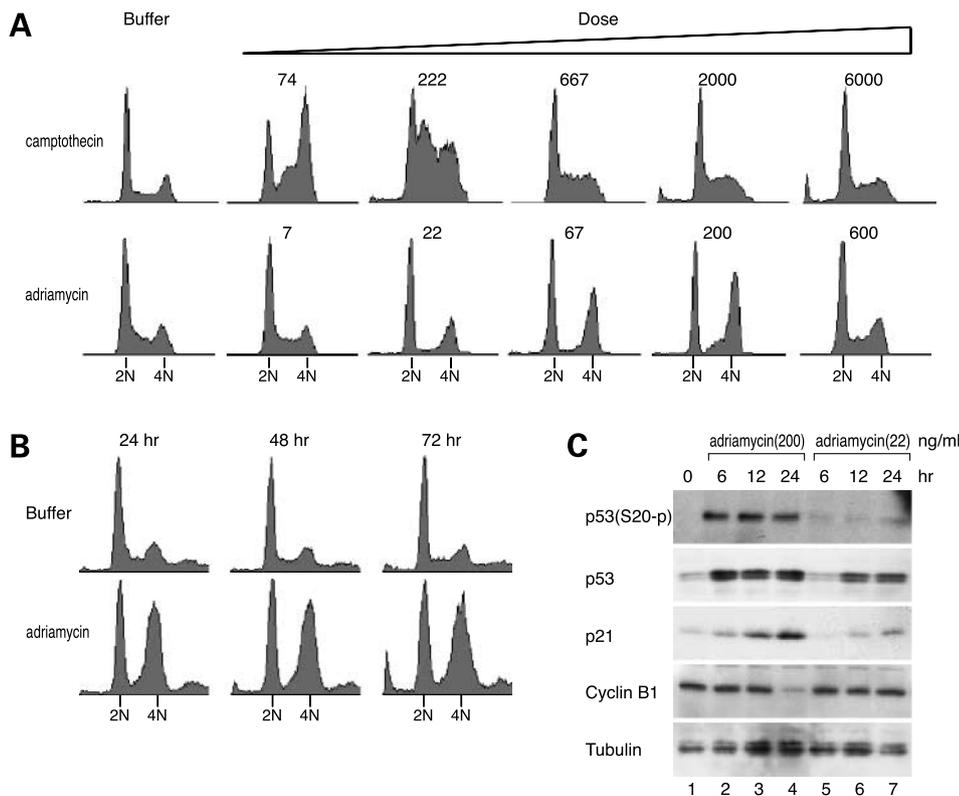
Figure 2. Different doses of Topo poisons differentially trigger multiple cell cycle arrest. **A,** cell cycle arrest induced by Topo poisons. HepG2 cells were mock treated or treated with the indicated concentrations of camptothecin or Adriamycin as in Fig. 1A. After 24 h, the cells were harvested for flow cytometry analysis (*abscissa,* DNA content; *ordinate,* cell number). The positions of 2N and 4N DNA contents are indicated. **B,** Adriamycin induces stable cell cycle arrest. HepG2 cells were mock treated or treated with 200 ng/ml of Adriamycin. Cells were harvested for flow cytometry analysis at the indicated time. **C,** temporal relationship between p53 activation and cyclin B1 down-regulation. HepG2 cells were treated with the indicated dose of Adriamycin, and cell extracts were prepared at the indicated time points. The relative abundance of Ser20-phosphorylated p53, p53, p21$^{CIP1/WAF1}$, and cyclin B1 was detected by immunoblotting. Immunoblotting for tubulin indicates similar sample loadings.

at Ser20, ahead of the decrease in cyclin B1. In accordance with the activation of p53, p21$^{CIP1/WAF1}$ was induced after p53. The inverse correlation between p53 activation and cyclin B1 is in line with the idea that p53 can repress the cyclin B1 promoter (39, 40). In contrast, p53 was only marginally activated (Ser20 phosphorylation was not detected) and cyclin B1 was not degraded at a lower dose of Adriamycin.

Taken together, these data show that the responses to Topo inhibitors differ substantially depending on the dosage. While inhibitory phosphorylation of cyclin-CDK complexes is prominent at relatively low doses of inhibitors, full activation of p53 (Ser20 phosphorylation and p21$^{CIP1/WAF1}$ induction) and down-regulation of cyclin B1 occur at high concentrations.

Caffeine Disrupts Multiple Topo Poisons-Induced DNA Damage Checkpoints

To see whether the responses to Adriamycin and camptothecin were mediated by ATM or related protein kinases, caffeine was added to uncouple these protein kinases (41–45). After Adriamycin treatment, pRb was inactivated and its gel mobility was shifted to the hypophosphorylated form (Fig. 3A). Hyperphosphorylation of pRb was restored by caffeine, suggesting that the Adriamycin-induced G$_1$ checkpoint is dependent on ATM/ATR. Moreover, the stabilization of p53 after Adriamycin treatment was abolished by caffeine (Fig. 4A).

To see whether the Topo poisons-induced S phase checkpoint is sensitive to caffeine, BrdUrd incorporation after DNA damage was examined. Treatment with caffeine

alone did not significantly alter the cell cycle distribution or BrdUrd uptake. A relatively low dose of camptothecin reduced the portion of cells incorporating BrdUrd from ~35% to ~20% (Fig. 3B). Significantly, caffeine suppressed the block of DNA synthesis and restored BrdUrd uptake to control level. In contrast, the decrease of BrdUrd incorporation after treatment with Adriamycin or higher concentration of camptothecin was not restored by caffeine. These data indicate that ATM and ATR may be involved in the inhibition of DNA synthesis after relatively modest level of DNA damage by camptothecin.

To see whether caffeine can circumvent the G$_2$ DNA damage checkpoint, the CDC2 activity and histone H3 phosphorylation after drug treatment were monitored. As expected, histone H3 phosphorylation at Ser10 (an event that normally occurs as cells enter prophase) diminished after incubation with either Adriamycin or camptothecin (Fig. 4A, compare to control in *lane 9*). Significantly, caffeine was able to promote histone H3 phosphorylation. Caffeine was less effective in cells treated with higher concentrations of Adriamycin or camptothecin. Similarly, caffeine stimulated the *in vitro* kinase activities of CDC2 (Fig. 4B). Again, caffeine was effective in activating CDC2 after low doses of Adriamycin and camptothecin, but not after treatment with high doses.

To see whether the histone H3 phosphorylation caused by caffeine was specific for a certain period during the cell cycle, we next analyzed histone H3 phosphorylation and DNA content simultaneously with flow cytometry (Fig. 4C). As expected with a normal growing population,

phosphorylated histone H3 was found exclusively in cells with 4N DNA content ($\sim 2\%$). Unexpectedly, while histone H3 phosphorylation was stimulated by caffeine in 4N cells, caffeine also promoted histone H3 phosphorylation in cells arrested in G_1 (after treatment with 22 ng/ml of Adriamycin). In accordance with the results from immunoblotting (Fig. 4A), histone H3 phosphorylation was not increased when caffeine was added to cells treated with higher concentrations of Adriamycin (Fig. 4C) or camptothecin (data not shown). This lack of effect of caffeine on histone H3 phosphorylation also served as a control to indicate that the increase in histone H3 phosphorylation signal was not due to non-specific antibody binding, DNA damage *per se*, or non-specific effects of caffeine. This is important as caffeine also increased histone H3 phosphorylation throughout the unperturbed cell cycle (Fig. 4C).

Collectively, these data indicate that caffeine can disrupt the Adriamycin- and camptothecin-induced DNA damage checkpoints in G_1 (as measured by pRb phosphorylation and p53 induction), S phase (as measured by DNA synthesis), and G_2 (as measured by histone H3 phosphorylation). Caffeine bypasses these checkpoints after moderate, but not severe level of DNA damage, implicating ATM and ATR as mediators of these checkpoints.
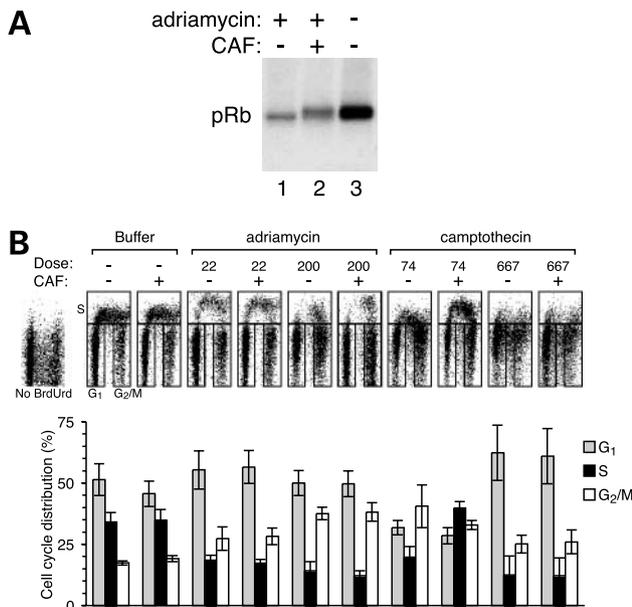

Figure 3. Caffeine uncouples the G_1 and S phase DNA damaging checkpoint. **A,** caffeine restores pRb phosphorylation after Adriamycin treatment. HepG2 cells were treated with either buffer (*lane 3*) or 67 ng/ml Adriamycin (*lanes 1* and *2*) for 24 h. Buffer (*lanes 1* and *3*) or caffeine (*CAF*; *lane 2*) was then added and the cells were incubated for a further 12 h. Cell extracts were prepared and pRb was detected by immunoblotting. **B,** caffeine promotes BrdUrd incorporation after camptothecin treatment. HepG2 cells were mock treated or treated with the indicated doses of camptothecin (nM) or Adriamycin (ng/ml) for 20 h as indicated. The cells were treated with buffer or caffeine for 3.5 h followed by BrdUrd labeling for 30 min. Flow cytometry profiles of BrdUrd incorporation (*ordinate*) and DNA content (*abscissa*) are shown. The profile of control cells without BrdUrd labeling is shown for reference. Cell cycle distribution (average and SD calculated from three independent experiments) is shown at the *bottom*. BrdUrd-positive cells were regarded as S phase cells.

The G_1 DNA Damage Responses to Topo Poisons Are Partially Dependent on ATM

To understand the role of ATM in Topo poisons-induced checkpoints, we next compared the responses of lymphoblastoid cells derived from AT or normal individuals. As expected, Adriamycin treatment reduced the S phase population in wild-type cells, which is indicative for cell cycle arrest in both G_1 and G_2 (Fig. 5A). In contrast, $ATM^{-/-}$ cells accumulated a 4N DNA content, suggesting that the Adriamycin-induced G_1 checkpoint was likely to be partially dependent on ATM. The defect of G_1 checkpoint in $ATM^{-/-}$ cells was further corroborated by the phosphorylation status of pRb (Fig. 5B). While the mobility shifts of pRb were abolished by Adriamycin in wild-type cells, the same treatment had no effect on pRb in $ATM^{-/-}$ cells.

To see whether the possible defect in Adriamycin-induced G_1 checkpoint correlated with p53 activation, the expression of p53 was examined in lymphoblastoid cells after Adriamycin treatment. Figure 6A shows that p53 was stabilized in both wild-type and $ATM^{-/-}$ cells by Adriamycin in a dose-dependent manner. However, it is notable that p53 was stabilized after treatment with relatively low doses of Adriamycin (7–22 ng/ml) in wild-type but not in $ATM^{-/-}$ cells (Fig. 6, A and B). In agreement with this, $p21^{CIP1/WAF1}$ was induced by 22 ng/ml of Adriamycin in wild-type but not in $ATM^{-/-}$ cells (Fig. 6B). Although p53 accumulated in both cell types after Adriamycin treatment, Ser20 was phosphorylated exclusively in wild-type cells (Fig. 6, A and B). These results indicate that ATM is essential for Ser20 phosphorylation of p53; ATM is required for the stabilization and activation of p53 at relatively low concentrations of Adriamycin, but not for higher Adriamycin concentrations.

As in HepG2 cells, CDC2(Thr14/Tyr15) phosphorylation occurred in lymphoblastoid cells at Adriamycin concentrations below that triggered full activation of p53 (Fig. 6A). Cyclin A and cyclin B1 were destroyed and CDC2 was dephosphorylated at higher concentrations of Adriamycin. Importantly, the pathways that lead to the inhibitory phosphorylation of CDC2 and the destruction of cyclins were unaffected by the status of ATM.

To see whether ATM accounts for the effects of caffeine on Adriamycin-induced responses (see Fig. 4A), caffeine was added to wild-type or $ATM^{-/-}$ lymphoblastoid cells following Adriamycin treatment. Figure 6B shows that caffeine significantly reduced the Adriamycin-induced p53 accumulation, Ser20 phosphorylation, and $p21^{CIP1/WAF1}$ induction in both wild-type and $ATM^{-/-}$ cells. These results suggest that both the ATM-dependent and -independent activation of p53 after Adriamycin treatment are caffeine sensitive.

Collectively, these data indicate that ATM is critical for p53 activation and the G_1 DNA damage checkpoint in response to Adriamycin. At higher concentrations of Adriamycin, however, the activation of p53 is ATM independent but is sensitive to caffeine.

Cells Lacking ATM Are Partially Defective in Campto-thecin-Induced S Phase DNA Damage Responses

We next investigated the role played by ATM in camptothecin-induced S phase checkpoint. Camptothecin delayed cell cycle progression in wild-type lymphoblastoid cells predominantly during S phase (Fig. 7A) (note that because lymphoblastoid cells were more sensitive to camptothecin than HepG2, a lower dose range of campto-thecin was used in these experiments). The intra-S checkpoint was confirmed by the decrease in BrdUrd uptake, in particular during later half of S phase (Fig. 8A). In marked contrast, a conspicuous defect in the S phase DNA damage checkpoint in ATM$^{-/-}$ cells was evidenced both from the accumulation of DNA content toward 4N (Fig. 7A) and the increase in BrdUrd incorporation (Fig. 8A). At higher concentrations of camptothecin (222 nM), both wild-type and ATM$^{-/-}$ cells were indistin-guishably arrested in early S phase (Fig. 7A), and less than 5% of cells incorporated BrdUrd (data not shown). These data indicate that the inhibition of DNA replication induced by camptothecin is in part dependent on ATM.

To see whether the defect of S phase response in ATM$^{-/-}$ cells correlated with protein expression, wild-type and ATM$^{-/-}$ cells were treated with different doses of camptothecin and harvested for immunoblotting. Figure 7B shows that the accumulation of p53 after camptothecin treatment was identical between wild-type and ATM$^{-/-}$ cells, suggesting that the faulty S phase DNA damage responses in ATM$^{-/-}$ cells were due to mechanisms other than p53. One such mechanism may be the inhibitory phosphorylation of CDK2, as the activation of CDK2 by recombinant CDC25A was weaker in ATM$^{-/-}$ cells than in wild-type cells (Fig. 7C). The decrease of CDK2 activity after camptothecin treatment was not due to a loss of its cyclin partner, because cyclin E accumulated as more cells were trapped in S phase with increasing dosage of camptothecin (Fig. 7B). These results suggest that inactiva-tion of CDK2 by Thr14/Tyr15 phosphorylation was defective in the absence of ATM.

Although ATM$^{-/-}$ cells were less responsive to campto-thecin than wild-type cells, DNA synthesis was clearly compromised after camptothecin treatment, especially
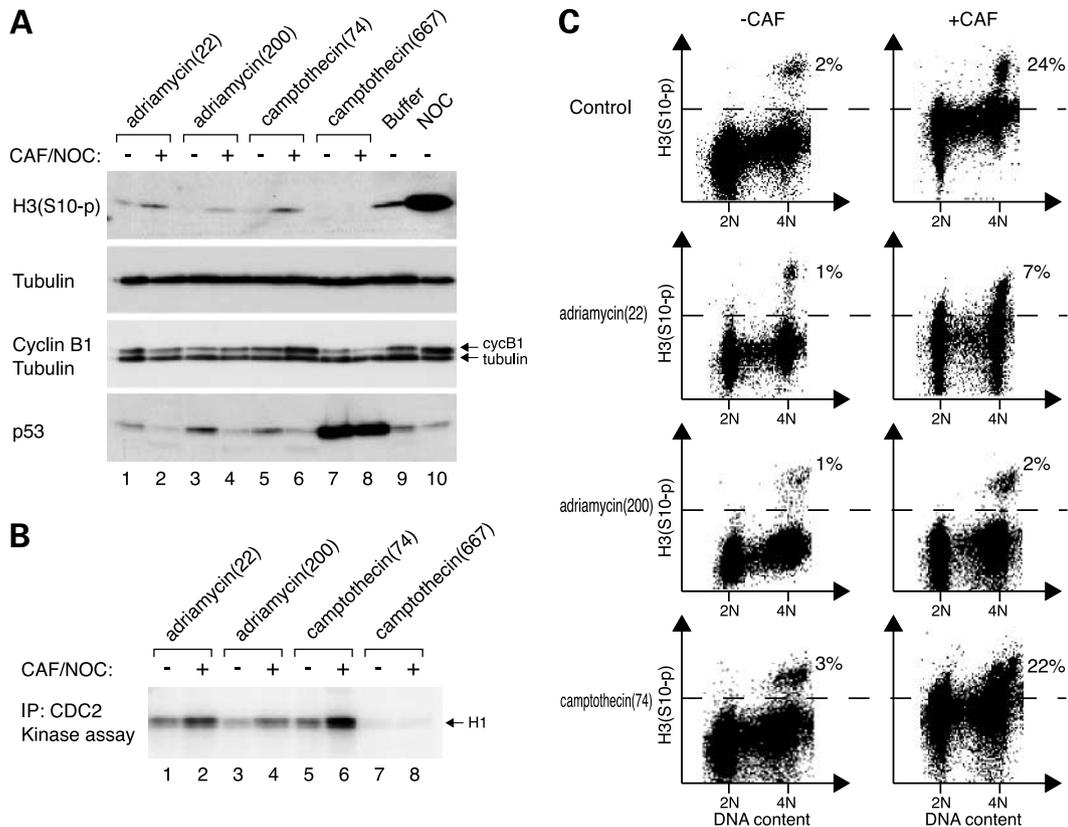

Figure 4.   Caffeine uncouples the G$_2$ checkpoint after moderate but not high level of DNA damage. **A,** HepG2 cells were treated with the indicated concentrations of Adriamycin (ng/ml) or camptothecin (nM) as indicated. After 20 h, cells were mock treated or treated with caffeine and nocodazole for another 6 h. Cell extracts were prepared and Ser10-phosphorylated histone H3, tubulin, cyclin B1, and p53 were detected by immunoblotting. Extracts from growing cells (*lane 9*) and nocodazole-blocked mitotic cells (*lane 10*) were included as controls for histone H3 phosphorylation. **B,** reactivation of CDC2 kinase activities by caffeine after DNA damage. Cell-free extracts (200 μg) from samples in panel **A** (*lanes 1–8*) were immunoprecipitated with antibodies against CDC2. The kinase activities against histone H1 were assayed and phosphorylation was detected with phosphorimagery. **C,** caffeine promotes histone H3 Ser10 phosphorylation throughout the cell cycle. HepG2 cells were treated with control buffer, Adriamycin (ng/ml), or camptothecin (nM) for 20 h. Cells were treated with buffer or caffeine for another 4 h. Cells were analyzed for Ser10-phosphorylated histone H3 (*ordinate*) and DNA content (*abscissa*) by flow cytometry. The percentage of cells containing phosphorylated histone H3 is indicated. The *dotted lines* indicate the cutoff level for background *versus* positive histone H3 phosphorylation signals.
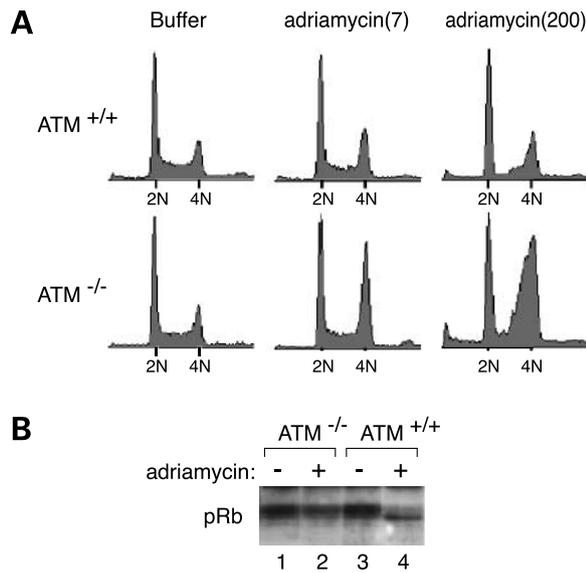
A

B

Figure 5. ATM is involved in G_1 cell cycle response to Adriamycin. **A,** G_1 cell cycle arrest induced by Adriamycin is defective in ATM$^{-/-}$ cells. Wild-type or ATM$^{-/-}$ lymphoblastoid cells were treated with buffer or the indicated doses of Adriamycin (ng/ml) for 24 h. Cell cycle distribution was analyzed by flow cytometry. **B,** ATM is required for the inhibition of pRb phosphorylation after DNA damage. ATM$^{-/-}$ or wild-type cells were treated with buffer or 67 ng/ml Adriamycin for 24 h as indicated. Cell extracts were prepared and pRb was detected by immunoblotting.

during the later part of S phase (Fig. 8A). To see whether this inhibition of replication is caffeine sensitive, BrdUrd incorporation assays were performed after caffeine treatment. As expected, caffeine restored DNA synthesis in wild-type cells after camptothecin-induced damage (Fig. 8A). Although caffeine did not statistically alter the percentage of BrdUrd-incorporating cells in the ATM$^{-/-}$ background, the extent of BrdUrd incorporation was appreciably increased in the presence of caffeine, especially for the later part of S phase. At a higher concentration of camptothecin (222 nM), caffeine was not able to restore BrdUrd uptake, irrespective of the status of ATM (data not shown). Collectively, these data indicate that the delay of S phase in response to camptothecin is compromised in the absence of ATM. ATM is not required for the activation of p53, but is involved in the inhibitory phosphorylation control of CDK2 after camptothecin treatment.

The Role of ATM in Topo Poisons-Induced Cell Death

To see whether mitosis was blocked after Topo poisons-induced damage, we have also examined histone H3 phosphorylation in lymphoblastoid cells. As in HepG2 (Fig. 1A), histone H3 phosphorylation diminished in lymphoblastoid cells treated with relatively low doses of Adriamycin (Fig. 6A) and camptothecin (Fig. 7B). However, histone H3 phosphorylation increased at higher concentrations of Adriamycin or camptothecin. This increase in histone H3 phosphorylation was peculiar for lymphoblastoid cells and was not observed in HepG2. We hypothesized that this may partly be due to apoptosis triggered by severe DNA damage in lymphoblastoid cells, as histone

H3 Ser10 phosphorylation has been reported to precede apoptosis in thymocytes (46, 47). In agreement with this idea, we found that cleavage of caspase-3 was triggered by Adriamycin (Fig. 6A) or camptothecin (Fig. 7B) in a
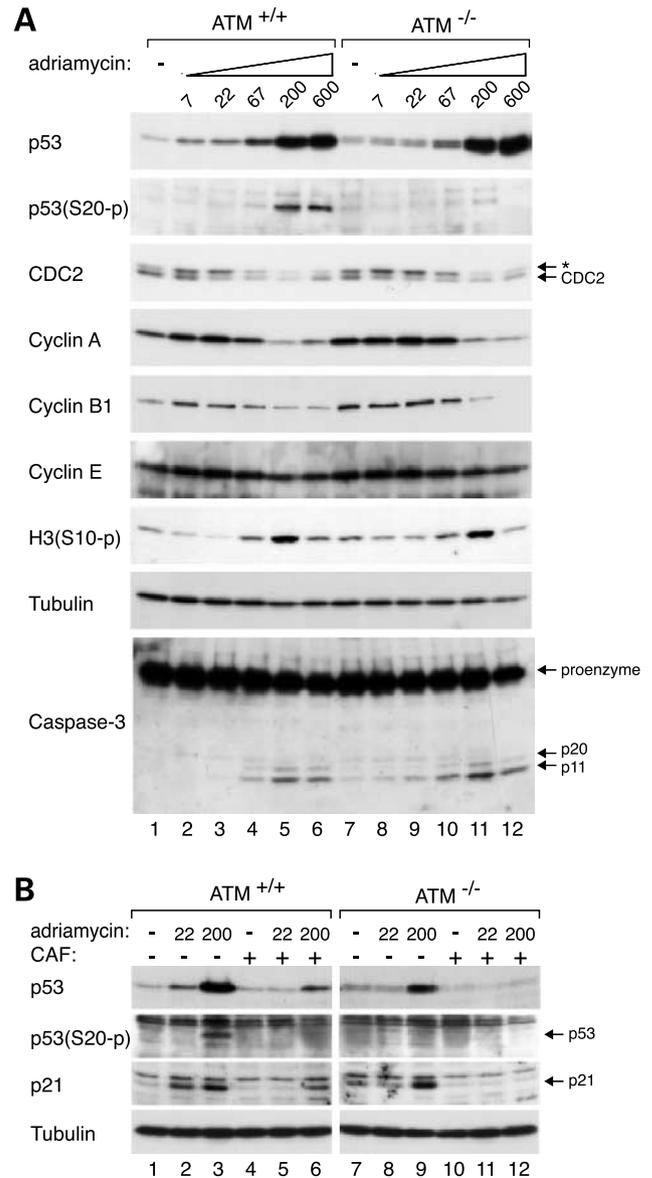
A

B

Figure 6. Accumulation of p53 and inactivation of CDC2 in response to Adriamycin are ATM independent. **A,** wild-type (*lanes 1–6*) or ATM$^{-/-}$ (*lanes 7–12*) lymphoblastoid cells were treated with buffer or the indicated doses of Adriamycin. Cell extracts were prepared and immunoblotted with antibodies against p53, Ser20-phosphorylated p53, CDC2, A-, B1-, and E-type cyclin, Ser10-phosphorylated histone H3, or caspase-3 as indicated. Constant level of protein loading was indicated by immunoblotting for tubulin. The *asterisk* indicates the position of the Thr14/Tyr15-phosphorylated forms of CDC2. The positions of the caspase-3 proenzyme and the cleavage products are indicated. **B,** bypass of Adriamycin-induced p53 and p21$^{CIP1/WAF1}$ by caffeine in ATM$^{-/-}$ cells. Wild-type or ATM$^{-/-}$ cells were treated with the indicated doses of Adriamycin (ng/ml) as indicated. After 20 h, cells were mock treated or treated with caffeine for another 6 h before cell extracts were prepared. The expression of p53, Ser20-phosphorylated p53, and p21$^{CIP1/WAF1}$ were detected by immunoblotting. Immunoblotting for tubulin indicates similar sample loadings.
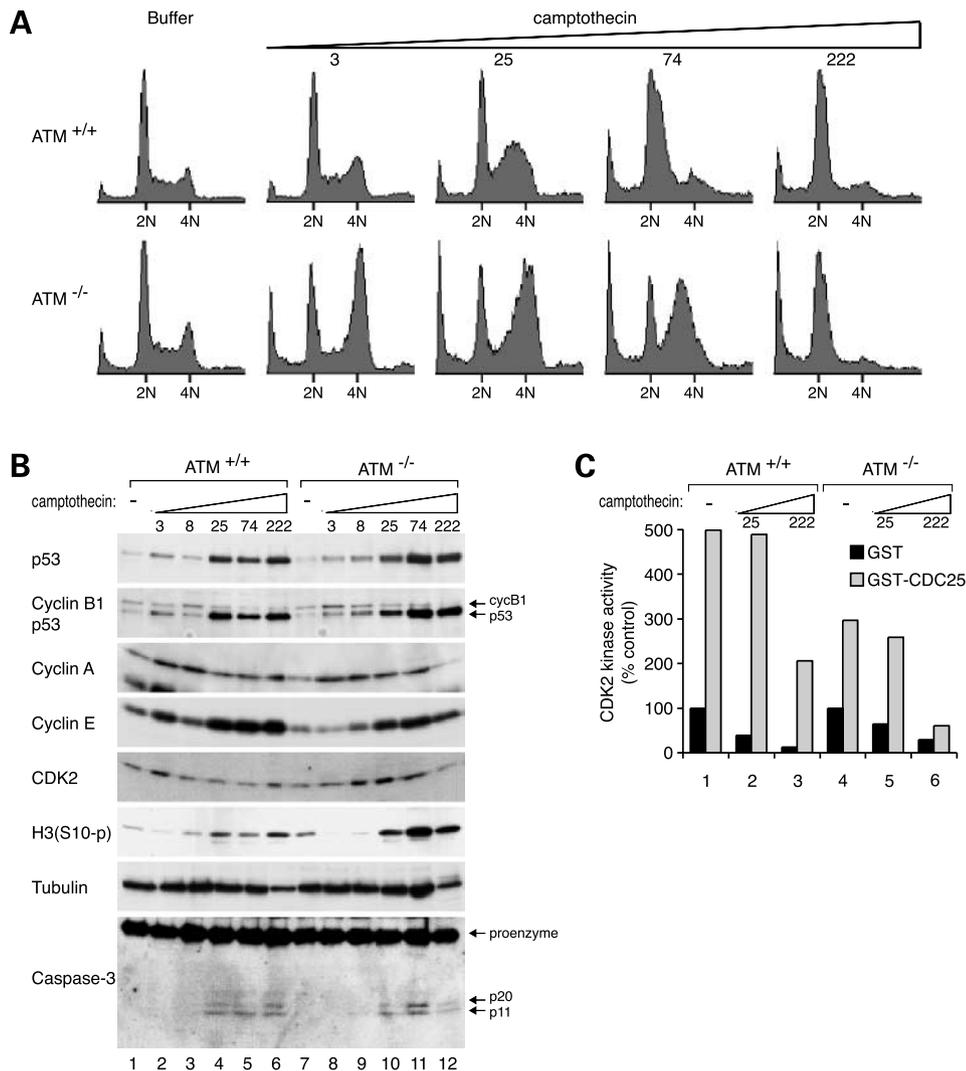
Figure 7. Cells lacking ATM are defective in S phase responses to camptothecin. **A,** ATM$^{-/-}$ cells are defective in camptothecin-induced S phase arrest. Wild-type or ATM$^{-/-}$ lymphoblastoid cells were treated with buffer or the indicated concentrations of camptothecin (nM) for 24 h. Cell cycle distribution was analyzed by flow cytometry. **B,** similar protein expression in wild-type and ATM$^{-/-}$ cells following camptothecin treatment. Wild-type (*lanes 1–6*) or ATM$^{-/-}$ (*lanes 7–12*) cells were treated with buffer or the indicated concentrations of camptothecin (nM). Cell extracts were prepared and immunoblotted with antibodies against p53, A-, B1-, and E-type cyclin, CDK2, Ser10-phosphorylated histone H3, or caspase-3 as indicated. The positions of the caspase-3 proenzyme and the cleavage products are indicated. Constant level of protein loading was indicated by immunoblotting for tubulin. **C,** reactivation of CDK2 by recombinant CDC25A in both wild-type and ATM$^{-/-}$ cells. Wild-type or ATM$^{-/-}$ cells were treated with buffer or with two doses of camptothecin (nM) as indicated. CDK2 was immunoprecipitated and incubated with either GST or GST-CDC25A as described in Materials and Methods. Histone H1 kinase activity was assayed and phosphorylation was quantified with phosphorimagery.

dose-dependent manner. Importantly, both wild-type and ATM$^{-/-}$ cells exhibited similar histone H3 phosphorylation and caspase-3 activation after DNA damage, suggesting that Topo poisons-induced apoptosis does not require ATM.

The Topo Poisons-Induced G$_2$ DNA Damage Checkpoint Is Independent on ATM

To see whether the Adriamycin-induced G$_2$ DNA damage checkpoint is dependent on ATM, the status of CDC2 was examined after Adriamycin treatment. CDC2 was phosphorylated after Adriamycin treatment in both wild-type and ATM$^{-/-}$ cells (Figs. 6A and 8B). Furthermore, the Adriamycin-induced CDC2 phosphorylation was abolished by caffeine in both backgrounds (Fig. 8B). Together with the results that the Adriamycin-induced G$_2$ cell cycle arrest was effective in ATM$^{-/-}$ cells (Fig. 5A), these data indicate that the Adriamycin-induced G$_2$ DNA damage checkpoint is ATM independent but caffeine sensitive.

Discussion

The basis of many anticancer therapies is the use of genotoxic agents that damage DNA and kill dividing cells.

Cells that contain intact DNA damage checkpoints are regarded to be more resistant to genotoxic stress because they can arrest the cell cycle and repair the damage. We show that several cell cycle checkpoints were activated by Topo I and Topo II poisons, depending on the dosage and cell type. Agents that override DNA damage checkpoints are of great interest because they are predicted to sensitize cells to DNA damaging agents. It is well established that caffeine can uncouple cell cycle progression from DNA replication and repair (48, 49). The best-characterized effect of caffeine is the overriding of the G$_2$ DNA damage checkpoint (50–52). Several lines of evidence indicate that ATM is an important target of caffeine (41–45). Interestingly, our data show that the G$_2$ DNA damage checkpoint induced by Topo poisons did not require ATM. In contrast, ATM played an important role in Topo poisons-induced G$_1$ and S phase checkpoints. See Table 1 for a summary of the checkpoint responses described in this study.

G$_1$ Checkpoint

A key mechanism for the G$_1$ checkpoint is the induction of p21$^{CIP1/WAF1}$ by p53 (53). It is puzzling that although

G_1 arrest was elicited at relatively low concentrations of Topo poisons, full accumulation of p53 and p21$^{CIP1/WAF1}$ was achieved only at higher drug concentrations (Figs. 1A, 6A, and 7B). One possibility is that a subtle induction of p21$^{CIP1/WAF1}$ (and the subsequent decrease in CDK2 activity) is sufficient to hinder G_1 progression. It is well established that phosphorylation of pRb by cyclin-CDK complexes is required for passage through the restriction point in late G_1 (reviewed in Ref. 54). As in the G_1 arrest induced by ionizing radiation (55), we found that Adriamycin inhibits the hyperphosphorylation of pRb in HepG2 (Fig. 3A) and lymphoblastoid cells (Fig. 5B).

A role for ATM/ATR in the G_1 checkpoint is suggested by the results that caffeine stimulated pRb phosphorylation (Fig. 3) and reduced the abundance of p53 (Fig. 4). More importantly, ATM$^{-/-}$ cells were defective in the G_1 delay (Fig. 5A), as well as regulation of pRb, p53, and p21$^{CIP1/WAF1}$ (Figs. 5B and 6B) after Adriamycin treatment. The defects in ATM$^{-/-}$ cells were limited to relatively low doses of Adriamycin. At higher doses of Adriamycin, induction of p53 and p21$^{CIP1/WAF1}$ occurred in both wild-type and ATM$^{-/-}$ cells, and was abolished by caffeine in both cell types (Fig. 6B). It should be noted that we could
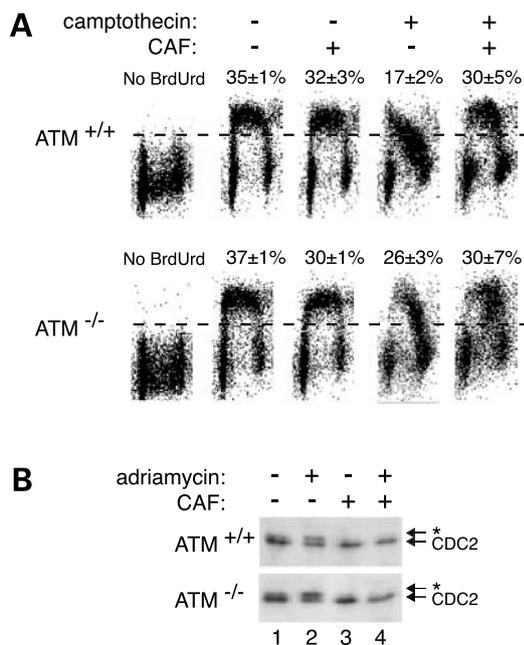

Figure 8. Bypass of Adriamycin- and camptothecin-induced DNA damage checkpoints by caffeine. **A,** BrdUrd incorporation in wild-type or ATM$^{-/-}$ lymphoblastoid cells. Cells were mock treated or treated with 25 nM camptothecin for 20 h. The cells were then incubated with caffeine for 3.5 h followed by BrdUrd labeling for 30 min. Flow cytometry profiles of BrdUrd incorporation (*ordinate*) and DNA content (*abscissa*) are shown. Control cells without BrdUrd labeling are shown for reference. The average and SD of the percentage of BrdUrd-positive cells (*dotted lines* indicate the cutoff) from three independent experiments are indicated. **B,** bypass of Adriamycin-induced CDC2 inactivation by caffeine in ATM$^{-/-}$ cells. Wild-type or ATM$^{-/-}$ cells were treated with buffer or 22 ng/ml of Adriamycin. After 20 h, cells were mock treated or treated with caffeine for another 6 h. Cell extracts were prepared and CDC2 was detected by immunoblotting. The *asterisk* indicates the position of the Thr14/Tyr15-phosphorylated forms of CDC2.

Table 1. Summary of ATM-dependent and -independent responses to Topo poisons

Topo Poison	Responses	ATM Dependence
Adriamycin	G_1 checkpoint:	
	↑ p53(Ser20)-p (high doses only)	Yes
	↑ p53	Yes (low doses only)
	↑ p21	Yes (low doses only)
	↓ pRb-p	Yes
	G_2 checkpoint:	
	↑ CDC2(T14/Y15)-p (low doses only)	No
	↓ cyclin B1 (high doses only)	No
	↓ histone H3(S10)-p	No
Camptothecin	Intra-S checkpoint:	
	↑ p53	No
	↑ CDK2(T1/Y15)-p	Yes (partial)
	↓ BrdUrd incorporation	Yes (partial)

not rule out the possibility that G_2 arrest was more effective in cells without ATM, hence reducing the relative G_1 population. It is interesting that although Ser20 phosphorylation was absolutely dependent on ATM, induction of p53 and p21$^{CIP1/WAF1}$ was defective only at relatively low doses of Adriamycin (Fig. 6A). Ser20 phosphorylation probably plays a minor role in the stabilization of p53 after Adriamycin-induced damage. Together, these results suggest that following severe DNA damage, activation of the p53-p21$^{CIP1/WAF1}$ pathway is maintained by an ATM-independent mechanism, involving ATR or other caffeine-sensitive proteins. In addition to inhibition by p21$^{CIP1/WAF1}$, a significant population of CDK2 was inhibited by Thr14/Ty15 phosphorylation after treatment with camptothecin (Figs. 1C and 7C) and Adriamycin.[1] Because CDK2 is involved in both G_1 (phosphorylation of pRb) and S phase (firing of replication origins and elongation, see below), inhibition of CDK2 has the potential for inhibition of both checkpoints.

Intra-S Checkpoint

Camptothecin causes double-strand DNA damage during replication (see ''Introduction''), which is reflected in the inhibition of DNA synthesis at the later part of S phase (Figs. 2A and 8A). Caffeine was effective in reactivating DNA replication after relatively mild but not severe camptothecin-induced DNA damage (Fig. 3B). The camptothecin-induced intra-S phase checkpoint was characterized by a decrease in BrdUrd incorporation in cells containing DNA content between 2N and 4N (Figs. 3B and 8A), indicating that DNA replication was inhibited after replication was initiated. In contrast, the DNA damage checkpoints in G_1 and G_2 induced by Adriamycin did not result in a BrdUrd-negative cell population between 2N and 4N (Fig. 3B). We found that ATM$^{-/-}$ cells were partially defective in the intra-S DNA replication

---

[1] Unpublished data.

block induced by camptothecin (Fig. 7A). This inhibition of DNA replication (in particular during late S phase) was still relieved by caffeine (Fig. 8A), which is consistent with the involvement of ATR as described by other studies (28, 29).

We found that the expression of p53 in response to camptothecin was not affected by the absence of ATM (Fig. 7B), suggesting that the defective intra-S checkpoint in $ATM^{-/-}$ cells may not be due to the p53-p21$^{CIP1/WAF1}$-CDK2 pathway. Similarly, the ionizing radiation-induced S phase checkpoint is also independent on p53 (56). Instead, ionizing radiation-induced S phase delay is enforced by an ATM-dependent mechanism involving the destruction of CDC25A followed by the inactivation of CDK2 (56–58). During replication, CDK2 is important for both origin activation and elongation (reviewed in Refs. 59, 60). Hence inhibition of CDK2 by camptothecin has the potential to both abolish origin activation and stall elongation of replicating DNA. However, because camptothecin induces DNA damage after initiation of replication, cells are likely to be arrested after the firing of some origins. This can be seen by the relatively normal BrdUrd incorporation in early S phase after camptothecin treatment (Figs. 3B and 8A). From the data described here, it is not clear whether late origins firing was inhibited after camptothecin treatment. This question is important because the answer would indicate whether the camptothecin-induced replication block represent a *bona fide* checkpoint. Our hypothesis is that inhibitory phosphorylation of CDK2 is also important for camptothecin-induced intra-S checkpoint and is defective in $ATM^{-/-}$ cells. We have recently shown that inhibitory phosphorylation plays a major role in the regulation of CDC2 but only a minor role for CDK2 during the unperturbed cell cycle of HeLa cells. After DNA damage and replication block, however, both CDC2 and CDK2 are inhibited by phosphorylation (32). In support of our hypothesis, the CDK2 inhibited after camptothecin treatment could be activated by recombinant CDC25A (Fig. 1C). We have previously shown that CDC25A is also rapidly destroyed after treatment with Topo poisons (61). Furthermore, we found that CDK2 was less sensitive to camptothecin in $ATM^{-/-}$ than in wild-type background (Fig. 7C and our unpublished observations). Finally, CDK2 from $ATM^{-/-}$ cells was less efficiently activated by CDC25A than that from wild-type cells (Fig. 7B). It would be interesting to see whether WEE1 and MYT1, the two protein kinases that phosphorylate CDK2, are also regulated by Topo poisons in an ATM-dependent manner.

G$_2$ Checkpoint

We previously showed that CDC2 is inactivated by Thr14/Tyr15 phosphorylation during Adriamycin-induced G$_2$ arrest (32, 38) (Fig. 1). Adriamycin-induced CDC2 phosphorylation was sensitive to caffeine but independent on ATM (Figs. 6A and 8B), explaining the presence of G$_2$-M arrest after Adriamycin treatment in $ATM^{-/-}$ cells (Fig. 5A). After more severe DNA damage, CDC2 was inactivated through down-regulation of cyclin B1 (Fig. 1), which also appears to be independent on ATM (Fig. 6A). The relative minor role of ATM in Adriamycin-induced G$_2$

arrest is in accord with the emerging evidence which indicate that ATR, rather than ATM, is the major player in the ionizing radiation-induced G$_2$ DNA damage checkpoint. Conditional disruption of ATR abolishes the majority of the ionizing radiation-induced G$_2$ arrest (5), especially for the late phase of the response (2–9 h post-ionizing radiation) (6).

We used phosphorylation of histone H3 at Ser10, which started during prophase and is required for proper chromosome condensation (62), as an indicator for G$_2$ checkpoint bypass. This is probably a reasonable assumption when the majority of the cells are indeed arrested in G$_2$. There are clearly important caveats to consider. First, caffeine stimulated histone H3 phosphorylation even in cells not containing 4N DNA (Fig. 4C). This is similar to our observations that ectopic expression of non-phosphorylatable CDC2 and CDK2 leads to unscheduled histone H3 phosphorylation throughout the cell cycle (32). Second, the increase in histone H3 phosphorylation may be transient.[2] Third, phosphorylation of histone H3 increased after DNA damage in some cell types like lymphoblastoid cells, most likely to be due to apoptosis (Figs. 6A and 7B). Extensive apoptosis was not observed for HepG2, as there was no increase in histone H3 phosphorylation (Fig. 1A) and caspase-3 activation (data not shown), and sub-G$_1$ population was not detected by flow cytometry (Fig. 2A). We think that the arguments for histone H3 phosphorylation as a measurement of G$_2$ bypass would likely be similar for other mitotic markers like MPM2 phosphorylation.

It is possible that the Adriamycin-induced mitotic delay described here is in part due to inhibition of decatenation rather than to DNA damage. Results obtained with the Topo II inhibitor ICRF-193 indicate that the decatenation checkpoint is enforced by ATR and BRCA1 (63). However, it has been subsequently shown that ICRF-193 is able to cause DNA damage under some conditions (64). The precise contribution of DNA damage and decatenation on the checkpoints described here is uncertain.

Although caffeine promoted CDC2 activation, histone H3 phosphorylation, and chromosome condensation in G$_2$-arrested cells, these cells never enter normal mitosis or beyond. Some authors have attributed this to an alternative pathway for G$_2$ arrest independently to the caffeine-sensitive pathway (65). It is possible that processes like the unscheduled histone H3 phosphorylation are detrimental to normal cell cycle progression. Understanding the precise involvement of ATM, ATR, or other proteins in different cell cycle checkpoints will be critical for the design of checkpoint-uncoupling agents for chemotherapies.

---

[2] Unpublished data.

References

1. Poon RYC. Cell cycle control. In: Bertino JR, editor. Encyclopedia of cancer. San Diego, CA: Academic Press; 2002. p. 393–404.

2. Shiloh Y. ATM and related protein kinases: safeguarding genome integrity. Nat Rev Cancer 2003;3:155–68.

3. Lavin MF, Shiloh Y. The genetic defect in ataxia-telangiectasia. Annu Rev Immunol 1997;15:177–202.

4. Nyberg KA, Michelson RJ, Putnam CW, Weinert TA. Toward maintaining the genome: DNA damage and replication checkpoints. Annu Rev Genet 2002;36:617–56.

5. Cortez D, Guntuku S, Qin J, Elledge SJ. ATR and ATRIP: partners in checkpoint signaling. Science 2001;294:1713–6.

6. Brown EJ, Baltimore D. Essential and dispensable roles of ATR in cell cycle arrest and genome maintenance. Genes Dev 2003;17:615–28.

7. Wang JY. Cancer. New link in a web of human genes. Nature 2000; 405:404–5.

8. Miyakawa Y, Matsushime H. Rapid downregulation of cyclin D1 mRNA and protein levels by ultraviolet irradiation in murine macrophage cells. Biochem Biophys Res Commun 2001;284:71–6.

9. Poon RYC, Toyoshima H, Hunter T. Redistribution of the CDK inhibitor p27 between different cyclin·CDK complexes in the mouse fibroblast cell cycle and in cells arrested with lovastatin or ultraviolet irradiation. Mol Biol Cell 1995;6:1197–213.

10. Agami R, Bernards R. Distinct initiation and maintenance mechanisms cooperate to induce G1 cell cycle arrest in response to DNA damage. Cell 2000;102:55–66.

11. Falck J, Mailand N, Syljuasen RG, Bartek J, Lukas J. The ATM-Chk2-Cdc25A checkpoint pathway guards against radioresistant DNA synthesis. Nature 2001;410:842–7.

12. Sorensen CS, Syljuasen RG, Falck J, et al. Chk1 regulates the S phase checkpoint by coupling the physiological turnover and ionizing radiation-induced accelerated proteolysis of Cdc25A. Cancer Cell 2003; 3:247–58.

13. Prives C. Signaling to p53: breaking the MDM2-p53 circuit. Cell 1998;95:5–8.

14. Saito S, Goodarzi AA, Higashimoto Y, et al. ATM mediates phosphorylation at multiple p53 sites, including Ser(46), in response to ionizing radiation. J Biol Chem 2002;277:12491–4.

15. Shieh SY, Ahn J, Tamai K, Taya Y, Prives C. The human homologs of checkpoint kinases Chk1 and Cds1 (Chk2) phosphorylate p53 at multiple DNA damage-inducible sites. Genes Dev 2000;14:289–300.

16. Hirao A, Kong YY, Matsuoka S, et al. DNA damage-induced activation of p53 by the checkpoint kinase Chk2. Science 2000;287:1824–7.

17. Chehab NH, Malikzay A, Appel M, Halazonetis TD. Chk2/hCds1 functions as a DNA damage checkpoint in G(1) by stabilizing p53. Genes Dev 2000;14:278–88.

18. Zhou BB, Elledge SJ. The DNA damage response: putting checkpoints in perspective. Nature 2000;408:433–9.

19. Lopez-Girona A, Kanoh J, Russell P. Nuclear exclusion of Cdc25 is not required for the DNA damage checkpoint in fission yeast. Curr Biol 2001;11:50–4.

20. Blasina A, de Weyer IV, Laus MC, Luyten WH, Parker AE, McGowan CH. A human homologue of the checkpoint kinase Cds1 directly inhibits Cdc25 phosphatase. Curr Biol 1999;9:1–10.

21. Mailand N, Podtelejnikov AV, Groth A, Mann M, Bartek J, Lukas J. Regulation of G(2)/M events by Cdc25A through phosphorylation-dependent modulation of its stability. EMBO J 2002;21:5911–20.

22. Lee J, Kumagai A, Dunphy WG. Positive regulation of Wee1 by Chk1 and 14-3-3 proteins. Mol Biol Cell 2001;12:551–63.

23. Bast RC, Kufe DW, Pollock RE, et al. Cancer medicine, 5th edition. Ontario, Canada: B.C. Decker Inc.; 2000.

24. Banin S, Moyal L, Shieh S, et al. Enhanced phosphorylation of p53 by ATM in response to DNA damage. Science 1998;281:1674–7.

25. Canman CE, Wolff AC, Chen CY, Fornace AJ Jr, Kastan MB. The p53-dependent G1 cell cycle checkpoint pathway and ataxia-telangiectasia. Cancer Res 1994;54:5054–8.

26. Ye R, Bodero A, Zhou BB, Khanna KK, Lavin MF, Lees-Miller SP. The plant isoflavenoid genistein activates p53 and Chk2 in an ATM-dependent manner. J Biol Chem 2001;276:4828–33.

27. Theard D, Coisy M, Ducommun B, Concannon P, Darbon JM. Etoposide and Adriamycin but not genistein can activate the checkpoint kinase Chk2 independently of ATM/ATR. Biochem Biophys Res Commun 2001;289:1199–204.

28. Wang H, Wang X, Zhou XY, et al. Ku affects the ataxia and Rad 3-related/CHK1-dependent S phase checkpoint response after campto-thecin treatment. Cancer Res 2002;62:2483–7.

29. Cliby WA, Lewis KA, Lilly KK, Kaufmann SH. S phase and G2 arrests induced by topoisomerase I poisons are dependent on ATR kinase function. J Biol Chem 2002;277:1599–606.

30. Arooz T, Yam CH, Siu WY, Lau A, Li KK, Poon RY. On the concentrations of cyclins and cyclin-dependent kinases in extracts of cultured human cells. Biochemistry 2000;39:9494–501.

31. Siu WY, Arooz T, Poon RYC. Differential responses of proliferating *versus* quiescent cells to Adriamycin. Exp Cell Res 1999;250:131–41.

32. Chow JPH, Siu WY, Ho HTB, Ma KHT, Ho CC, Poon RYC. Differential contribution of inhibitory phosphorylation of CDC2 and CDK2 for unperturbed cell cycle control and DNA integrity checkpoints. J Biol Chem 2003;278:40815–28.

33. Poon RYC, Hunter T. Dephosphorylation of Cdk2 Thr^{160} by the cyclin-dependent kinase-interacting phosphatase KAP in the absence of cyclin. Science 1995;270:90–3.

34. Li KKW, Ng IOL, Fan ST, Albrecht JH, Yamashita K, Poon RYC. Activation of cyclin-dependent kinases CDC2 and CDK2 in hepatocellular carcinoma. Liver 2002;22:259–68.

35. Puisieux A, Galvin K, Troalen F, et al. Retinoblastoma and p53 tumor suppressor genes in human hepatoma cell lines. FASEB J 1993; 7:1407–13.

36. Chehab NH, Malikzay A, Stavridi ES, Halazonetis TD. Phosphorylation of Ser-20 mediates stabilization of human p53 in response to DNA damage. Proc Natl Acad Sci USA 1999;96:13777–82.

37. Shieh SY, Taya Y, Prives C. DNA damage-inducible phosphorylation of p53 at N-terminal sites including a novel site, Ser20, requires tetramerization. EMBO J 1999;18:1815–23.

38. Poon RYC, Chau MS, Yamashita K, Hunter T. The role of Cdc2 feedback loop control in the DNA damage checkpoint in mammalian cells. Cancer Res 1997;57:5168–78.

39. Innocente SA, Abrahamson JL, Cogswell JP, Lee JM. p53 regulates a G2 checkpoint through cyclin B1. Proc Natl Acad Sci USA 1999;96: 2147–52.

40. Passalaris TM, Benanti JA, Gewin L, Kiyono T, Galloway DA. The G(2) checkpoint is maintained by redundant pathways. Mol Cell Biol 1999;19:5872–81.

41. Zhou BB, Chaturvedi P, Spring K, et al. Caffeine abolishes the mammalian G(2)/M DNA damage checkpoint by inhibiting ataxia-telangiectasia-mutated kinase activity. J Biol Chem 2000;275:10342–8.

42. Moser BA, Brondello JM, Baber-Furnari B, Russell P. Mechanism of caffeine-induced checkpoint override in fission yeast. Mol Cell Biol 2000;20:4288–94.

43. Blasina A, Price BD, Turenne GA, McGowan CH. Caffeine inhibits the checkpoint kinase ATM. Curr Biol 1999;9:1135–8.

44. Sarkaria JN, Busby EC, Tibbetts RS, et al. Inhibition of ATM and ATR kinase activities by the radiosensitizing agent, caffeine. Cancer Res 1999;59:4375–82.

45. Hall-Jackson CA, Cross DA, Morrice N, Smythe C. ATR is a caffeine-sensitive, DNA-activated protein kinase with a substrate specificity distinct from DNA-PK. Oncogene 1999;18:6707–13.

46. Waring P, Khan T, Sjaarda A. Apoptosis induced by gliotoxin is preceded by phosphorylation of histone H3 and enhanced sensitivity of chromatin to nuclease digestion. J Biol Chem 1997;272:17929–36.

47. Enomoto R, Koyamazaki R, Maruta Y, et al. Phosphorylation of histones triggers DNA fragmentation in thymocyte undergoing apoptosis induced by protein phosphatase inhibitors. Mol Cell Biol Res Commun 2001;4:276–81.

48. Schlegel R, Pardee AB. Caffeine-induced uncoupling of mitosis from the completion of DNA replication in mammalian cells. Science 1986;232: 1264–6.

49. Lau CC, Pardee AB. Mechanism by which caffeine potentiates lethality of nitrogen mustard. Proc Natl Acad Sci USA 1982;79:2942–6.

50. Walters RA, Gurley LR, Tobey RA. Effects of caffeine on radiation-induced phenomena associated with cell-cycle traverse of mammalian cells. Biophys J 1974;14:99–118.

51. Rowley R, Zorch M, Leeper DB. Effect of caffeine on radiation-induced

mitotic delay: delayed expression of G2 arrest. Radiat Res 1984;97: 178 – 85.

52. Rowley R. Reduction of radiation-induced G2 arrest by caffeine. Radiat Res 1992;129:224 – 7.

53. Poon RYC, Jiang W, Toyoshima H, Hunter T. Cyclin-dependent kinases are inactivated by a combination of p21 and Thr-14/Tyr-15 phosphorylation after UV-induced DNA damage. J Biol Chem 1996;271:13283 – 91.

54. Harbour JW, Dean DC. The Rb/E2F pathway: expanding roles and emerging paradigms. Genes Dev 2000;14:2393 – 409.

55. Khanna KK, Beamish H, Yan J, et al. Nature of G1/S cell cycle checkpoint defect in ataxia-telangiectasia. Oncogene 1995;11:609 – 18.

56. Xie G, Habbersett RC, Jia Y, et al. Requirements for p53 and the ATM gene product in the regulation of G1/S and S phase checkpoints. Oncogene 1998;16:721 – 36.

57. Mailand N, Falck J, Lukas C, et al. Rapid destruction of human Cdc25A in response to DNA damage. Science 2000;288:1425 – 9.

58. Beamish H, Williams R, Chen P, Lavin MF. Defect in multiple cell cycle checkpoints in ataxia-telangiectasia postirradiation. J Biol Chem 1996; 271:20486 – 93.

59. Bell SP, Dutta A. DNA replication in eukaryotic cells. Annu Rev Biochem 2002;71:333 – 74.

60. Yam CH, Fung TK, Poon RYC. Cyclin A in cell cycle control and cancer. Cell Mol Life Sci 2002;59:1317 – 26.

61. Chow JPH, Siu WI, Fung TK, et al. DNA damage during the spindle-assembly checkpoint degrades CDC25A, inhibits cyclin-CDC2 complexes, and reverses cells to interphase. Mol Biol Cell 2003;14:3189 – 4002.

62. Wei Y, Yu L, Bowen J, Gorovsky MA, Allis CD. Phosphorylation of histone H3 is required for proper chromosome condensation and segregation. Cell 1999;97:99 – 109.

63. Deming PB, Cistulli CA, Zhao H, et al. The human decatenation checkpoint. Proc Natl Acad Sci USA 2001;98:12044 – 9.

64. Mikhailov A, Cole RW, Rieder CL. DNA damage during mitosis in human cells delays the metaphase/anaphase transition via the spindle-assembly checkpoint. Curr Biol 2002;12:1797 – 806.

65. Barratt RA, Kao G, McKenna WG, Kuang J, Muschel RJ. The G2 block induced by DNA damage: a caffeine-resistant component independent of Cdc25C, MPM-2 phosphorylation, and H1 kinase activity. Cancer Res 1998;58:2639 – 45.

Molecular Cancer Therapeutics

Topoisomerase poisons differentially activate DNA damage checkpoints through ataxia-telangiectasia mutated–dependent and –independent mechanisms

Wai Yi Siu, Anita Lau, Talha Arooz, et al.

Updated version	Access the most recent version of this article at: http://mct.aacrjournals.org/content/3/5/621

Cited articles	This article cites 62 articles, 33 of which you can access for free at: http://mct.aacrjournals.org/content/3/5/621.full#ref-list-1
Citing articles	This article has been cited by 17 HighWire-hosted articles. Access the articles at: http://mct.aacrjournals.org/content/3/5/621.full#related-urls

E-mail alerts	Sign up to receive free email-alerts related to this article or journal.
Reprints and Subscriptions	To order reprints of this article or to subscribe to the journal, contact the AACR Publications Department at pubs@aacr.org.
Permissions	To request permission to re-use all or part of this article, use this link http://mct.aacrjournals.org/content/3/5/621. Click on "Request Permissions" which will take you to the Copyright Clearance Center's (CCC) Rightslink site.